Chapter 13.
Modification of surfaces with calix[4]arene diazonium salts

Ludovic Troian-Gautier, Alice Mattiuzzi, Pascale Blond, Maurice Retout, Gilles Bruylants, Olivia Reinaud, Corinne Lagrost and Ivan Jabin*

* *Corresponding Author:* Ivan.Jabin@ulb.be

L. Troian-Gautier, P. Blond, I. Jabin*
Laboratoire de Chimie Organique, Service de Chimie et PhysicoChimie Organiques, Université libre de Bruxelles (ULB), Avenue F.D. Roosevelt 50, CP160/06, 1050 Brussels, Belgium.

A. Mattiuzzi
X4C, 128 Rue du chêne Bonnet, 6110 Montigny-le-tilleul, Belgium

M. Retout, G. Bruylants
Engineering of Molecular NanoSystems, Ecole Polytechnique de Bruxelles, Université libre de Bruxelles (ULB), Avenue F. D. Roosevelt 50, CP165/64, B-1050 Brussels, Belgium.

O. Reinaud
Laboratoire de Chimie et de Biochimie Pharmacologiques et Toxicologiques, CNRS UMR 8601, Université de Paris, 45 rue des Saints Pères, 75006 Paris, France.

C. Lagrost
Université de Rennes, CNRS, ISCR-UMR 6226, F-35000 Rennes, France.

Abstract

Since their first report in 2012, calix[4]arene tetradiazonium derivatives have experienced a growing interest. They now represent a favored method to obtain robust post-functionalizable monolayers with controlled composition on a wealth of surfaces (conductive, semi-conductive or insulating, as well on large surfaces as on nanomaterials). These compounds are easily synthesized and handled and, so far, have been used to functionalize surfaces for applications in (bio)sensing, catalysis, as well as for the development of hydrophobic or antifouling coatings. This chapter describes the current synthetic methods, applications and limitations of these polydiazonium salts and discusses the potential of the field.

13.1 Introduction

Calix[n]arenes are oligomeric macrocycles composed of "n" *para*-substituted phenolic units (with n = 4, 6 or 8 being the most common) linked in the *ortho* position through methylene bridges.[1] Amongst the so-called 'remarkable' conformations in solution,[2] the "cone"

conformation, with its well-defined small and large rims, represents an attractive candidate for surface functionalization using diazonium chemistry. Especially, calix[4]arenes offer a rigid cone-constrained structure with a small rim composed of phenolic units which are particularly suited for the easy introduction of functional groups whereas the large rim can be selectively functionalized to introduce diazonium groups. Surface functionalization with molecular macrocycles including calixarenes, cyclodextrins, cucurbiturils have already been reported notably from self-assembly procedures [3, 4] in order to develop sensors where the molecular cavities defined by the structure of the macrocycles were employed for trapping analytes. Yet, the preparation of functional surfaces with well-ordered and robust structures, an aspect that has hardly been realized in the field, is of great importance in many applications including (bio-)sensors, molecular electronics, precision engineering, etc. Patterning surfaces with organic thin films through reductive diazonium grafting constitutes an attractive approach in this context because of the high robustness of the resulting interface and the large choice of materials that can be modified, both in terms of nature and forms. While many approaches are limited to a few types of materials, diazonium can be grafted on a very wide range of materials: metals (even oxidizable ones), carbon under various allotropic forms, polymers, semi-conductors, oxides, glasses, etc.[5, 6]

However, in some applications, nanostructured ultrathin films are required, and the formation of dense and organized monolayers or ultrathin films are particularly difficult to control through diazonium grafting. Indeed, the grafting process involves highly reactive radicals that are able to bind various substrates, but that are also able to react with already grafted organic moieties, leading to loosely packed aryl multilayers of 10-15 nm thickness. Several strategies have been proposed to produce well-ordered monolayers as recently reviewed.[7, 8] The use of calix[4]arenes represents an original approach to reach a structuring of the interface at the molecular scale.[9-11] The methylene bridges at the ortho position of the phenoxy substituents efficiently prevent the radical reaction responsible for the formation of multilayers. The possible functionalization of the small rim allows the introduction of various chemical function with a spatial control imposed by the geometry of the rim. The spatial arrangement of functional groups at the interface has been less considered than the control of monolayers formation and robustness of the interface but may be crucial in some applications. The rigid structure of calix[4]arene allows very good lateral and spatial controls of interfacial functionality.[12] Another key point is the cone-constrained structure that orients all the diazonium functions at the large rim in the same direction. This specific design is expected to enhance the stability of the monolayers thanks to multiple anchoring points, as evidenced with

the self-assembly of multipodal ligands.[13] In this chapter, we describe the synthesis of calix[4]arenes-tetradiazonium salts and their use as highly versatile platforms for surface modification able to bring robust and precise control of functionality of many materials including nanomaterials. The interest of the strategy is finally illustrated by a few examples of applications involving the calix[4]arene-based coatings.

13.2 Synthesis of calix[4]arene tetradiazonium derivatives

Most of the calix[4]arene tetradiazonium derivatives have been synthesized through a common route that involves i) an alkylation of the phenol units of *p-t*Bu-calix[4]arene, ii) an *ipso*-nitration reaction, iii) a reduction of the resulting nitro groups into the corresponding amines, and finally iv) a diazotization reaction. The synthesis of a calix[4]arene bearing a single diazonium group was also reported according to a slightly different strategy.[14] Selective introduction of different functional groups on the small rim can be readily achieved through strategies that are well-known in the field of calix[4]arene chemistry.[15] It is important to mention that substituents larger than an ethyl group have to be introduced on the phenol positions in order to prevent "*through the anulus*" rotation of the aromatic units and thus lock the calix[4]arene in the required cone conformation. The tetradiazonium salts that have been reported so far (*i.e.* **1**-**12**) are represented in **Figure 1**. All these compounds were easily characterized by NMR and IR spectroscopy and stored in the fridge for months without any noticeable degradation.

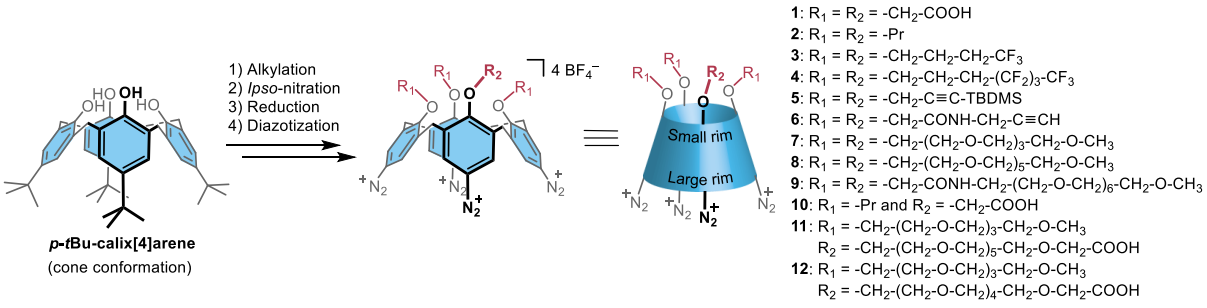

Figure 1. Structures of calix[4]arene tetradiazonium derivatives **1**-**12**.[9, 10, 14, 16-21]

13.3 Surface modification and characterization

Surface modification with calix[4]arene derivatives was achieved on conductive (glassy carbon, pyrolyzed photoresist films (PPF), gold), semi-conductive (germanium) and insulating (glass, polypropylene, polyethylene terephthalate, polystyrene) surfaces, as well as on metallic nanoparticles (**Figure 2**).[9, 10, 14, 16-21] The modified surfaces were characterized by several

techniques including electrochemistry, atomic force microscopy (AFM), X-Ray photoelectron spectroscopy (XPS), ellipsometry or infrared spectroscopy.[9, 10, 16, 18-21] In all cases, a dense, robust and homogeneous monolayer of calix[4]arenes was observed.

In the case of conductive surfaces, electrochemical reduction of the calixarene tetradiazonium derivatives was achieved either through cyclic voltammetry, where the potential is cycled through a range of potentials that include the reduction potential of the diazonium moiety, or through chronoamperometry, where a potential more negative than the reduction potential of the diazonium moiety is applied. The electrochemical reduction leads to the formation of aryl radicals at the vicinity of the electrode, resulting in an efficient grafting at the surface of the conductive electrode. Surface modification can be assessed through several methods, but most commonly, electrochemistry with redox probes such as dopamine or potassium ferricyanide is used.[22] Indeed, the thin layer of calix[4]arenes, if homogeneous, creates a barrier that significantly slows down the electron transfer kinetics at the interface. Experimentally, the efficient grafting is evidenced by a drastic decrease of current intensity along with an increased peak-to-peak separation between redox peaks (**Figure 2**).

Reducing agents such as $NaBH_4$ or sodium ascorbate were used for the grafting of calixarene tetradiazonium derivatives on nanoparticles. For example, $NaBH_4$ was used to obtain calix[4]arene-coated gold nanoparticles (AuNPs-calix), either formed *in situ* from (H/K)$AuCl_4$ or through ligand exchange of citrate-capped AuNPs.[20, 21, 23] Another chemical approach relies on the formation of intermediate diazoates through the reaction between diazonium derivatives and sodium hydroxide. This was used to covalently immobilize calix[4]arenes **1** and **3** onto gold, polypropylene, polyethylene terephthalate and polystyrene materials.[19] Similar procedures were used to functionalize glass, gold and polypropylene surfaces with calix[4]arene **4**[24] or germanium surfaces with calix[4]arenes **7**, **8** and **11**.[16] In the specific case of calix[4]arene **4**, a mixture of CH_3CN/aq. NaOH (0.1M) was used as it maximized solubility of the polyfluorinated calix[4]arene **4**, while still allowing the generation of diazoates by reaction with sodium hydroxide.

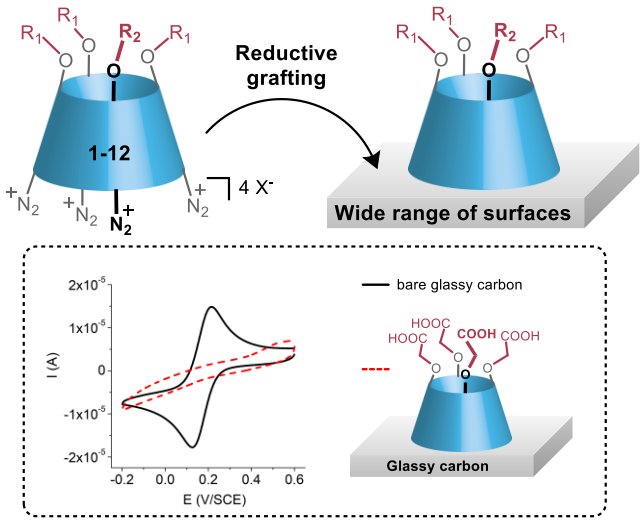

Figure 2. Grafting of calixarene tetradiazonium derivatives **1-12** on surfaces. The inset shows the cyclic voltammetry of $[Fe(CN)_6]^{3-}$ (1mM) on bare (black) and modified (red) glassy carbon in aqueous 0.5M KPF_6 recorded at 100 $mV.s^{-1}$.

13.3.1 Formation of true monolayers

The formation of true monolayers may be crucial for some applications such as (bio)sensing or electrocatalysis. Both of these applications require fast (electronic) communication between the sensitive layer and the analyte or compound to activate. Typical aryl diazonium derivatives, unless specific approaches are used,[7, 8] form multi-layers by reaction of the corresponding reactive radicals in solution with already grafted aryl groups. In the case of calix[4]arene tetradiazonium salts, the methylene bridges linking the different phenol units efficiently prevent further side reactions with the macrocyclic scaffold, once these are grafted on a surface. The formation of true monolayers is thus obtained. Ellipsometry and AFM scratching experiments were used to confirm the formation of monolayers of calix[4]arenes **1**, **3**, **4**, **7** and **8** on gold, germanium, PPF and polypropylene surfaces.[10, 16, 19] As a representative example, a thickness of 1.3±0.1 nm (AFM) and 1.09 ±0.2 nm (ellipsometry) was measured for a layer of calix[4]arene **3** on gold surfaces, which is in close agreement with the theoretical value of 1.1 nm estimated from MM2 energy minimizations.[10]

13.3.2 Formation of mixed monolayers of controlled composition

Functionalizing surfaces with different organic molecules in controlled ratios represents a promising, yet challenging endeavor. Control over the surface chemical composition can, for example, have a drastic impact on the sensitivity of a biosensor. Indeed, diluting the component of recognition can increase sensitivity by improving accessibility of the analyte.[25, 26] In addition, a combination of the properties of the individual organic molecules is expected to be

transferred on the surfaces when mixed layers are formed. Chemisorption of organic molecules in mixed ratios, such as thiols, is a possible approach, but it suffers from several limitations: i) surface coverage may differ from solution composition due to different adsorption kinetics,[27-29] and ii) inhomogeneity at the surface may result from segregation upon self-assembly.[30, 31] Thoroughly investigated on surfaces, this difficulty to control the layer composition has also been demonstrated on nanomaterials.[32] The formation of mixed layers of aryl diazonium derivatives in controlled ratios is also challenging. Indeed, the most easily reduced diazonium derivative is usually found in a larger ratio on the surface than in solution.[33, 34]

The formation of a mixed monolayer with a controlled composition represents another breakthrough, which was made possible through the use of calix[4]arene tetradiazonium derivatives. Indeed, the common macrocyclic scaffold roughly insulates the diazonium groups from the rest of the molecule and, as a result, the reduction potentials of all the calix[4]arene tetradiazonium salts are quite close. As a representative example, mixtures of calix[4]arenes **1** and **3** (in ratios of 100/0, 50/50, 10/90 and 0/100) were grafted using chronoamperometry at a applied potential of –0.5 V vs SCE for 5 minutes.[18] Control over the composition of the resulting mixed layers was then evidenced through determination of the static contact angle. The angle gradually increased from 68 ± 3° to 89 ± 2°, as the proportion of non-polar calix[4]arene **3** used in the grafting mixture increased. The formation of mixed monolayers was also achieved using $NaBH_4$ on gold nanoparticles with calix[4]arenes **1** and **9** in ratios 0/100, 5/95, 10/90, 25/75, 50/50, and 100/0.[21] Attenuated total reflectance Fourier transform infrared (ATR-FTIR) spectroscopy confirmed that the solution ratio was effectively transferred onto the surface, through the analysis of characteristic IR absorbance bands (asymmetric COC stretching at 1105 cm^{-1} as well as amide I at 1669 cm^{-1} and amide II at 1540 cm^{-1} for calix[4]arene **9** and asymmetric (1604 cm^{-1}) and symmetric (1420 cm^{-1}) COO^- stretching for calix[4]arene **1**).

13.3.3 Post-functionalization of calixarene-based monolayers

A particular benefit of using calix[4]arene derivatives is that the small rim can be substituted with groups particularly suited for post-functionalization (*i.e.* functionalization of the calixarenes once grafted), such as carboxyl, azide and alkyne.[9, 10, 17-21] Therefore, the covalent immobilization of various (bio)molecules can be achieved under classical conjugation reaction conditions. For example, amino containing compounds were anchored to grafted calixarenes bearing carboxyl groups (*i.e.* **1**, **11** and **12**) via classical peptide-type coupling reactions. This strategy was used to conjugate small amines or alcohols,[19, 20] as well as larger

peptides or proteins.[35, 36] Besides, click chemistry allowed the conjugation of azido-containing molecules on calixarene-based layers bearing alkynes groups. [17]

13.3.4 Robustness of the calixarene-based coatings

Calix[4]arene tetradiazonium salts display four anchoring points and can thus potentially form up to four links with the surface. This leads to a remarkable stability of the calixarene-based coating that outperform that of other classical organic coatings (SAMs of thiols, aryldiazoniums, etc.). This stability is notably assessed by the aggressive post-grafting workup that includes several washing cycles under sonication in various solvents (e.g. water, EtOH, DCM, ACN, THF, 0.1 M HCl, toluene, etc.). In the specific case of germanium surfaces modified by calix[4]arenes **7** and **8**, a continuous 10 µL/min flow of PBS-D_2O buffer over 16 hours was used. The IR spectra recorded at intervals during these 16 hours were superimposable, confirming the robustness of the grafted layer. The increased stability is particularly striking on nanomaterials.[20, 21] Indeed, typical gold nanoparticles stabilized by citrate readily degrade or aggregate due to changes in pH, ionic strength, or in the presence of large concentration of fluoride. In contrast, calixarene-coated gold nanoparticles such as AuNPs-calix**1** remained stable upon extreme pH variations, in the presence of large concentrations of fluoride ions (between 0.15 and 0.75 M) or when the ionic strength was increased (**Figure 3**).[20, 21] Even more remarkably, AuNPs-calix**1** could be completely dried, yielding a gold-colored film, and then resuspended into a 0.1 M aqueous NaOH solution. This unique stability conferred by calixarene-based coatings was exploited for the synthesis of silver and alloyed gold-silver nanoparticles.[23] These nanomaterials are particularly attracting in the biosensing field due to the enhanced optical properties of silver in comparison to gold.

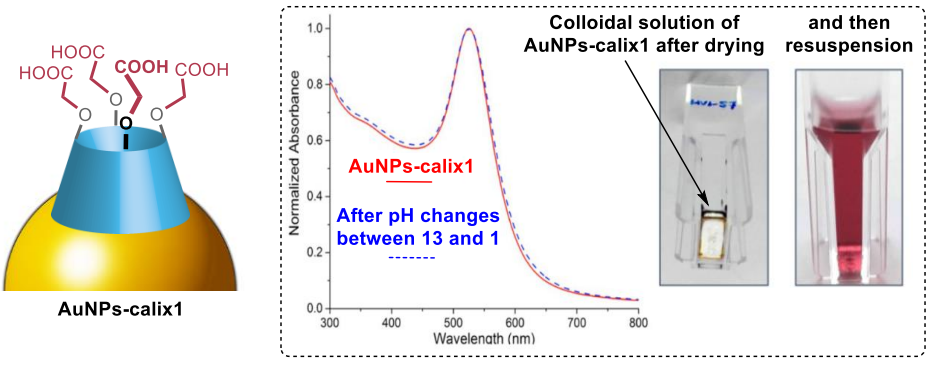

Figure 3. Schematic representation of AuNPs coated with calix[4]arene **1** (AuNPs-calix1). Inset: normalized UV-Visible absorption spectra of AuNPs-calix1 after several pH changes between 13 and 1

(left). Dried AuNPs-calix1 and resuspended in 0.1 M aqueous NaOH (right). Reproduced with permission from reference [20]. Copyright (2016) Royal Society of Chemistry.

13.4 Applications of calix[4]arene tetradiazonium-based coatings

The use of calix[4]arene tetradiazonium derivatives has already found applications in the fields of dewetting,[24] antifouling,[16] (bio)sensing,[16, 17] and electrocatalysis.[37]

13.4.1 Hydrophobicity

Exerting control over wettability[38-40] is a highly relevant endeavor for the development of coatings for anti-frosting and anti-fogging,[41, 42] self-cleaning,[43] anti-corrosion,[44, 45] or antibiofouling surfaces.[16, 46] The wettability is assessed by static contact angle measurements. Glass, gold and polypropylene surfaces were covalently modified with a polyfluorinated calix[4]arene tetradiazonium salt (**4**) (**Figure 4**).[24] A chemical grafting was performed using CH_3CN/0.1M NaOH aqueous solution. For gold surfaces, the grafting of **4** was also performed electrochemically for comparisons purposes. The modified surfaces displayed significant changes in static contact angles that evolved from 24.6 ± 2.0°, 64.7 ± 2.1° and 102.9 ± 3.9° to 110.0 ± 1.8°, 113.7 ± 2.2° and 112.6 ± 4.0° for glass, gold and polypropylene surfaces, respectively. These values are not far from the maximum value of 120° that has been estimated for smooth surfaces. Importantly, the coatings remained stable for at least 18 months, as the static contact angles for the aged surfaces were within 5% of the values obtained for freshly modified ones. Such a result is remarkable regarding ultrathin coatings.

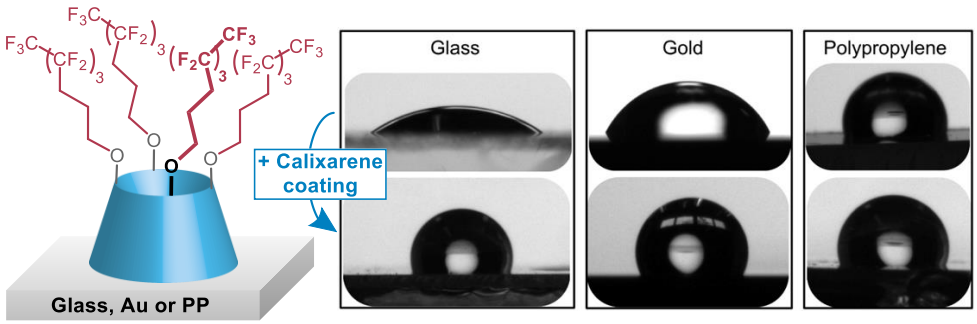

Figure 4. Left: schematic representation of the surfaces modified with calixarene **4**. Images of 2µL water droplets in contact with (top) bare glass, gold and polypropylene surfaces and with (bottom) the same surfaces freshly modified with calix[4]arene **4**. Reproduced with permission from reference [24]. Copyright (2020) Royal Society of Chemistry.

13.4.2 Antifouling

Germanium prisms displaying antifouling properties were developed with the aim of designing ATR-FTIR biosensors (*vide supra*). For this, calix[4]arene tetradiazonium salts substituted with oligo-(ethylene glycol) (oEGs) chains (*i.e.* **7** and **8**) were used, as oEGs are

known to be non-toxic and non-immunogenic, as well as to prevent the non-specific adsorption of biomolecules. The efficient grafting was confirmed by AFM and ATR-FTIR measurements, where the typical asymmetric COC stretching (1100 cm^{-1}) from the oEG chains, together with the symmetric COCAr stretching (from 1050 to 1020 cm^{-1}) and the aromatic ring stretching (1460 cm^{-1}) were observed. The non-specific adsorption of bovine serum albumin (BSA) was then investigated in phosphate buffer media in D_2O (PBS-D_2O) at 22 °C. With an unmodified germanium prism, the non-specific adsorption of BSA was clearly observed through increased absorbance signals corresponding to the amide-I', C=O(ND) stretching vibrations and amide-II' in plane ND bending vibrations measured at 1640 cm^{-1} and 1450 cm^{-1}, respectively. Astoundingly, the non-specific adsorption of BSA was prevented by more than 85% with the calix[4]arene-coated germanium prism.

13.4.3 Sensing

13.4.3.1 Electrochemical sensing in water

Gold electrodes were covalently modified with calix[4]arene **1** and a post-functionalization reaction with propargylamine allowed the introduction of alkyne groups on the surface.[17] A calix[6]arene-based copper *funnel* complex was then conjugated through an electro-click reaction. Funnel complexes are efficient receptors for neutral molecules and mimic the active site of metallo-enzymes by exhibiting a hydrophobic cavity associated to a confined metal center.[47] The resulting sensor was then used for the selective electrochemical detection of primary amines at µM concentrations in aqueous and organic solutions, where the electrochemical signal of the $Cu^{II/I}$ couple was shown to shift by 100 mV upon binding the amine derivative (**Figure 5**). Interestingly, the sensor was selective towards primary linear alkylamines that can access to the metal center through the calix[6]arene cavity.

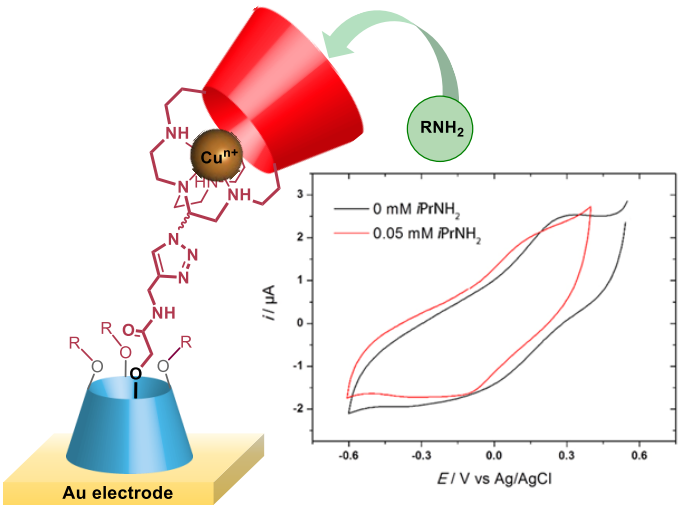

Figure 5. Selective electrochemical sensing of primary amines on gold electrodes using a calix[6]arene $Cu^{II/I}$ funnel complex. Reproduced with permission from ref [17]. Copyright (2016) American Chemical Society.

13.4.3.2 FTIR detection of proteins in biological media

Detection of proteins in complex media can be performed by Fourier transform infrared (FTIR) spectroscopy.[48] One advantage of this technique is that a multitude of biophysical and chemical information can be obtained from the IR signature of proteins (*i.e.* identification of their secondary and tertiary structures, post-translational modifications, etc.).[49] ATR FTIR-based biosensors make use of an organic layer, directly grafted onto the internal reflection element, to which a biological receptor is bound.[50] Germanium is particularly suitable for these applications. In this context, the grafting of stable, dense, and thin organic layers on germanium surfaces was recently accomplished through the reductive grafting of calix[4]arene-tetradiazonium salts.[16] Calix[4]arene **11** was specifically designed to decrease nonspecific adsorption thanks to oEG chains while the introduction of a carboxyl group allows for bioconjugation to a recognition unit.[35] Germanium surfaces modified with calix[4]arene **11** were converted to the corresponding activated esters using EDC/NHS prior to being conjugated to a biotin derivative bearing a terminal amino group (**Figure 6**). The resulting calix[4]arene-biotin-based germanium biosensors were then used to detect streptavidin (SA) (100 µg/mL) from a complex medium by ATR-FTIR spectroscopy. Bound SA was identified through the characteristic amide-I and amide-II IR absorption bands at 1637 cm^{-1} and 1535 cm^{-1}, respectively (**Figure 6a**). The location of these IR absorption bands indicated that SA was bound in its native β-sheet conformation. Recognition was also effective with streptavidin in the presence of bovine serum albumin (BSA) (100 µg/mL). Very interestingly, following incubation, BSA is not detected in the IR spectra, which highlights the remarkable antifouling properties of the calixarene-coated germanium surfaces. Similar strategies were also developed using fluorescent streptavidin-ATTO655, for which the specific interaction with biotin-spotted germanium surface generated a fluorescent microarray corresponding to the immobilized biotin pattern (**Figure 6b**).

Altogether, these results indicated that surface modification with a calix[4]arene-based platform allowed immobilization of receptors that retain their recognition properties and could selectively detect a protein in a medium containing other proteins such as BSA. Additional strong points of this strategy are i) the possibility to identify the secondary structure, ii) the small quantity of material necessary for the analysis (1µL of solution, 100 µg/mL) and iii) the analysis time (1 minute by IR spectra).

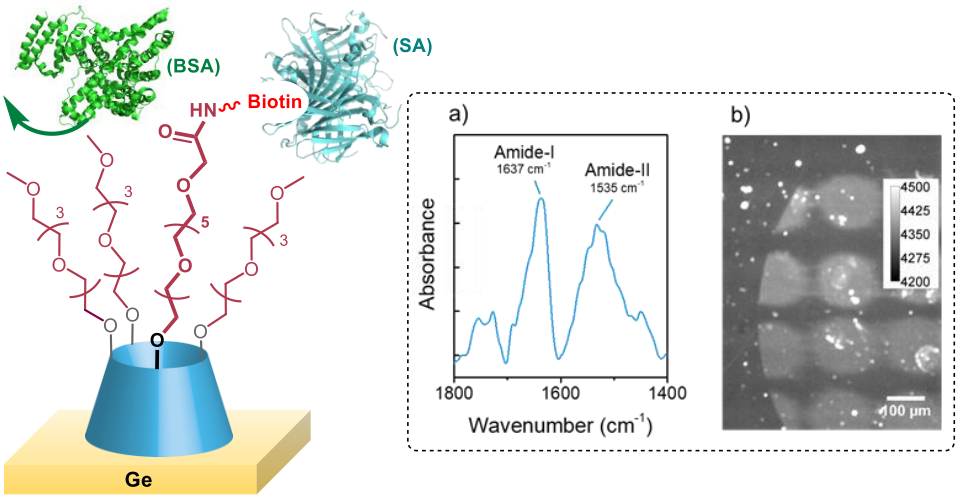

Figure 6. FTIR-based selective biosensor for streptavidin (SA) composed of a calix[4]arene-biotin-based germanium surface. Inset: a) ATR-FTIR adsorption spectra obtained after incubation in a solution of SA; b) Fluorescence image acquired on Ge-calix[4]arene-biotin spotted surface that was incubated with fluorescent streptavidin ATTO-655. The microarray's interstices, where incubation was carried out but biotin is not immobilized, served as a control area to evaluate the SA nonspecific adsorption, which was extremely limited according to the very weak fluorescence intensity in these regions. Reproduced with permission from ref [35]. Copyright (2020) American Chemical Society.

13.4.3.3 Calix[4]arene-coated gold nanoparticles for sensing of MDM2 in biological media

Gold nanoparticles are often employed as colorimetric indicators for *in vitro* diagnostic systems due to their optical properties. These NP have to be functionalizable, in order to allow coupling of specific recognition ligands, and their colloidal suspension must be stable in the operating medium (*i.e.* serum). The grafting on AuNPs is mostly relying on the well-known sulfur-gold interaction. However, control over the bioconjugation density represents a major challenge with thiol chemistry.[32] In this context, controlled bioconjugation of peptide aptamers and sensing of a cancer biomarker, *i.e.* the oncoprotein Mdm2, were recently obtained using calix[4]arene-coated AuNPs.[36] Firstly, AuNPs coated with a dense and stable oEG layer displaying carboxyl groups were readily obtained by using mixtures of calixarenes **7** and **12**. The resulting AuNPs-calix were shown to be more resistant to physical stress, such as temperature increase or drying, than related thiolated AuNPs. The high stability of the AuNPs-calix enabled their dispersion in human serum without any aggregation or degradation. The carboxyl terminal groups of the calixarene-based layer were used to conjugate amino-containing molecules via the formation of amide bonds. Control over the bioconjugation density was demonstrated by the conjugation of a cyanine7.5 dye to different batches of AuNPs

prepared with different mixtures of calixarenes **7** and **12**. As shown by UV-Vis spectroscopy, the density of the conjugated dye was proportional to the amount of calix[4]arene **12** used during the modification of the AuNPs, showing that the calixarene-based strategy is suitable for controlling the conjugation density of (bio)molecules on AuNPs. This approach was extended to the conjugation of peptides aptamers. It is remarkable that a positively charged aptamer could be grafted on the particles with a defined density without loss of colloidal stability, which was proven impossible with the classical thiol chemistry on citrate capped AuNPs.[51] Once modified, the resulting AuNPs were used for the detection of Mdm2 via a dual-trapping strategy (**Figure 7a**), leading to an aggregation of the AuNPs which was then quantified by UV-Vis spectroscopy. The aggregation intensity was shown to be proportional to the concentration of Mdm2 present at the AuNP interface (**Figure 7b**). This confirmed that biomolecules such as peptide aptamers can be covalently conjugated on the oEG shell of calixarenes-modified AuNPs in a controlled way, without any loss of their recognition abilities.

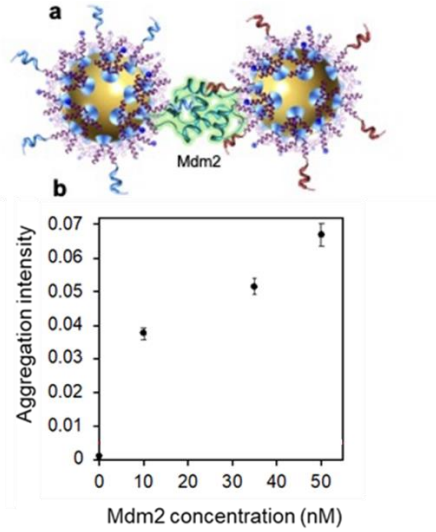

Figure 7. (a) Illustration of the dual-trapping of Mdm2 by calixarene-coated AuNPs. (b) Aggregation intensity of calixarene-coated AuNPs as a function of Mdm2 concentration. Reproduced with permission from ref [36]. Copyright (2021) American Chemical Society.

13.4.4 Electrocatalysis

Oxygen reduction reaction (ORR) is one of the most important reactions for technologies related to energy conversion. However, it is a complex, multi-electron process, exhibiting sluggish kinetics and, without a suitable catalyst, ORR occurs at high overpotentials. The direct, 4-electron reduction, which produces water, is generally the most desired route, while the 2-electron ORR pathway results in the formation of hydrogen peroxide. Additionally, the catalysts can also strongly influence product selectivity by favoring specific reaction pathways. As efficient catalysts, noble metal nanomaterials have been extensively developed

with variations of their size, shape and topmost layer composition in order to enhance their efficiency, durability and selectivity. More recently, the deliberate surface modification of nanocatalysts with organic ligands has emerged as a promising strategy to increase the electrocatalytic performance,[52, 53] AuNPs have been shown to act as catalysts for the ORR in alkaline media, mainly through an indirect ($2e^- + 2e^-$) pathway.[54] In this context, gold nanoparticles of 6 nm diameter coated with a monolayer of covalently-bound calix[4]arene **1** (AuNPs-**1**) showed enhanced selectivity and stability compared to AuNPs classically stabilized by citrate (AuNPs-citrate).[37] Rotating-ring disk electrode (RRDE) measurements allowed the monitoring of the number of electrons exchanged (*n*) together with the proportion of hydrogen peroxide formed during the process (%H_2O_2). While AuNPs-citrate displayed the expected $2e^- + 2e^-$ catalytic mechanism, the calix[4]arene-gold nanohybrids showed a constant value of *n* (3.9) and very low level of %H_2O_2 (% HO_2-< 5 %) over a large range of potentials (0.8 V to – 0.4 V vs RHE) (**Figure 8**). AuNPs-**1** clearly exhibit an enhanced selectivity toward the 4-electron pathway, close to what is currently obtained with the archetypal Pt ORR nanocatalysts but in acidic media. The kinetic current density and onset potential (~ 0.9 V vs RHE) compared well with reported specific activities of noble metal electrocatalysts, both bare and chemically modified.[37] Interestingly, the Tafel plots at low current density (close to the onset potential) were found to have a slope of 42 mV/decade, which is close to the value reported for bare 5 nm AuNPs, but substantially lower than the 60 mV /decade usually observed for metallic catalysts. This value indicates superior activity of the hybrid nanocatalysts.[55] Accelerated durability tests highlighted the robustness of AuNPs-**1** under operation. No variation of the linear sweep voltammograms (LSV) were observed after 1000 cycles in an aqueous 0.1 M KOH O_2-saturated solution. Additionally, X-ray photoelectron spectroscopy analyses further confirmed the robustness of the nanohybrid catalysts as the chemical footprint of the catalytic system remained intact in contrast to AuNPs-citrate that underwent chemical degradation. This strategy is expected to be further developed by modifying the small rim functionalities and the nature of the metallic core.

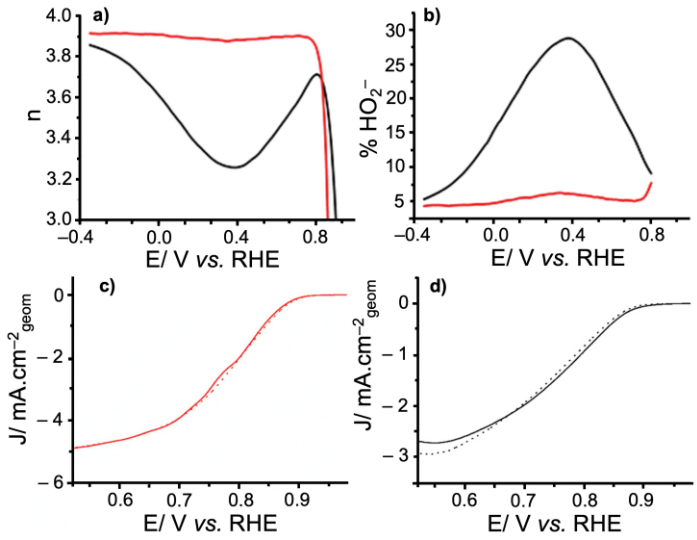

Figure 8. RRDE measurements showing a) the variation of n (number of exchanged electrons) and b) $\%HO_2^-$ (proportion of H_2O_2 produced) during ORR process for AuNPs-calix1 (red line) and AuNPs-citrate (black line). LSV curves before (dotted lines) and after (solid lines) the accelerated durability tests for c) AuNPs-calix1 and d) AuNPs-citrate. Reproduced with permission for ref [37]. Copyright (2021) John Wiley and Sons.

13.5 Conclusions and future perspectives

This chapter describes the use of calix[4]arene tetradiazonium derivatives constrained in a cone conformation as rigid 4-feeted platforms that present pre-/post-functionalizable arms. The synthesis of the platform is relatively straightforward and scalable. One side of the truncated cone (large rim of the calix[4]arene) is easily functionalized by amino groups that are ideal precursors for diazonium grafting, whereas the other side (small rim) can be pre- or post-functionalized almost at will to introduce specific functions. The large rim is used for the up-to-4-point grafting through the diazonium strategy, which yields the formation of strong chemical bonds with the surface. The molecular structure of the platform prevents the pitfalls of oligomerization during the grafting process that is usually observed with standard aryl-diazonium derivatives. This guarantees the formation of clean, compact, robust, dense monolayers on a great variety of materials. The optimal diazonium grafting procedure depends on the material and a variety of procedures have thus been developed for metal, polymers, glass surfaces of different size and shape. One of the most spectacular achievement is the formation of highly stable gold nanoparticles that do not irreversibly coalesce upon drying or with changes in pH or ionic strength. In addition, mixed monolayers of controlled composition are readily obtained when a mixture of two different calix[4]arene platforms with different arm functionalities for the grafting process is used.

Several applications benefiting from these calix[4]arene monolayers have already been reported. These include: i) the development of hydrophobic surfaces with perfluorinated groups grafted at the small rim, ii) the development of germanium surfaces for protein sensing and antifouling, iii) the electrochemical sensing or primary amines in water, iv) the recognition of MDM2 in biological media using a gold nanoparticles based colorimetric sensor and v) the controlled electrocatalysis of oxygen reduction.

Given their huge potential in the field of surface modification, we believe that calix[4]arene tetradiazonium salts will find many applications that could be exploited at the industrial level.

References

1. Gutsche CD. Calixarenes Revisited, Monographs in Supramolecular Chemistry. Cambridge: The Royal Society of Chemistry; 1998.
2. Ikeda A, Shinkai S (1997) Chem Rev 97:1713-34. doi: 10.1021/cr960385x.
3. Li H, Yang Y-W (2013) Chinese Chemical Letters 24:545-52. doi: 10.1016/j.cclet.2013.04.014.
4. Montes-García V, Pérez-Juste J, Pastoriza-Santos I, Liz-Marzán LM (2014) Chem Eur J 20:10874-83. doi: 10.1002/chem.201403107.
5. Bélanger D, Pinson J (2011) Chem Soc Rev 40:3995-4048. doi: 10.1039/C0CS00149J.
6. Berisha A, Chehimi MM, Pinson J, Podvorica F. Electrode Surface modification using diazonium salts. In: Bard AJ, Zoski CG, editors. Electroanalytical chemistry, a series of advances Boca Raton: CRC Press, Taylor & Francis group; 2016.
7. Breton T, Downard AJ (2017) Australian Journal of Chemistry 70:960-72. doi: 10.1071/CH17262.
8. Mattiuzzi A, Lenne Q, Carvalho Padilha J, Troian-Gautier L, Leroux YR, Jabin I, Lagrost C (2020) Frontiers in Chemistry 8. doi: 10.3389/fchem.2020.00559.
9. Buttress JP, Day DP, Courtney JM, Lawrence EJ, Hughes DL, Blagg RJ, Crossley A, Matthews SE, Redshaw C, Bulman Page PC, Wildgoose GG (2016) Langmuir 32:7806-13. doi: 10.1021/acs.langmuir.6b02222.
10. Mattiuzzi A, Jabin I, Mangeney C, Roux C, Reinaud O, Santos L, Bergamini J-F, Hapiot P, Lagrost C (2012) Nat Commun 3:1130. doi: 10.1038/ncomms2121.
11. Troian-Gautier L, Mattiuzzi A, Reinaud O, Lagrost C, Jabin I (2020) Organic & Biomolecular Chemistry 18:3624-37. doi: 10.1039/D0OB00070A.
12. Valášek M, Mayor M (2017) Chem Eur J 23:13538-48. doi: 10.1002/chem.201703349.
13. Li Z-Q, Tang J-H, Zhong Y-W (2019) Chem Asian J 14:3119-26. doi: 10.1002/asia.201900989.
14. Malytskyi V, Troian-Gautier L, Mattiuzzi A, Lambotte S, Cornelio B, Lagrost C, Jabin I (2018) Eur J Org Chem 2018:6590-5. doi: doi:10.1002/ejoc.201801253.
15. Lavendomme R, Zahim S, De Leener G, Inthasot A, Mattiuzzi A, Luhmer M, Reinaud O, Jabin I (2015) Asian Journal of Organic Chemistry 4:710-22. doi: 10.1002/ajoc.201500178.
16. Blond P, Mattiuzzi A, Valkenier H, Troian-Gautier L, Bergamini J-F, Doneux T, Goormaghtigh E, Raussens V, Jabin I (2018) Langmuir 34:6021-7. doi: 10.1021/acs.langmuir.8b00464.

17. De Leener G, Evoung-Evoung F, Lascaux A, Mertens J, Porras-Gutierrez AG, Le Poul N, Lagrost C, Over D, Leroux YR, Reniers F, Hapiot P, Le Mest Y, Jabin I, Reinaud O (2016) J Am Chem Soc 138:12841-53. doi: 10.1021/jacs.6b05317.
18. Santos L, Mattiuzzi A, Jabin I, Vandencasteele N, Reniers F, Reinaud O, Hapiot P, Lhenry S, Leroux Y, Lagrost C (2014) J Phys Chem C 118:15919-28. doi: 10.1021/jp5052003.
19. Troian-Gautier L, Martínez-Tong DE, Hubert J, Reniers F, Sferrazza M, Mattiuzzi A, Lagrost C, Jabin I (2016) J Phys Chem C 120:22936-45. doi: 10.1021/acs.jpcc.6b06143.
20. Troian-Gautier L, Valkenier H, Mattiuzzi A, Jabin I, den Brande NV, Mele BV, Hubert J, Reniers F, Bruylants G, Lagrost C, Leroux Y (2016) Chem Commun 52:10493-6. doi: 10.1039/C6CC04534K.
21. Valkenier H, Malytskyi V, Blond P, Retout M, Mattiuzzi A, Goole J, Raussens V, Jabin I, Bruylants G (2017) Langmuir 33:8253-9. doi: 10.1021/acs.langmuir.7b02140.
22. DuVall SH, McCreery RL (1999) Anal Chem 71:4594-602. doi: 10.1021/ac990399d.
23. Retout M, Jabin I, Bruylants G (2021) ACS Omega 6: 19675-84. doi: 10.1021/acsomega.1c02327.
24. Mattiuzzi A, Troian-Gautier L, Mertens J, Reniers F, Bergamini J-F, Lenne Q, Lagrost C, Jabin I (2020) RSC Adv 10:13553-61. doi: 10.1039/D0RA01011A.
25. Liu, Gooding JJ (2006) Langmuir 22:7421-30. doi: 10.1021/la0607510.
26. Khor SM, Liu G, Fairman C, Iyengar SG, Gooding JJ (2011) Biosens Bioelectron 26:2038-44. doi: 10.1016/j.bios.2010.08.082.
27. Laibinis PE, Fox MA, Folkers JP, Whitesides GM (1991) Langmuir 7:3167-73. doi: 10.1021/la00060a041.
28. Laibinis PE, Nuzzo RG, Whitesides GM (1992) J Phys Chem 96:5097-105. doi: 10.1021/j100191a065.
29. Love JC, Estroff LA, Kriebel JK, Nuzzo RG, Whitesides GM (2005) Chem Rev 105:1103-70. doi: 10.1021/cr0300789.
30. Stranick SJ, Parikh AN, Tao YT, Allara DL, Weiss PS (1994) J Phys Chem 98:7636-46. doi: 10.1021/j100082a040.
31. Imabayashi S-i, Hobara D, Kakiuchi T, Knoll W (1997) Langmuir 13:4502-4. doi: 10.1021/la970447u.
32. Retout M, Brunetti E, Valkenier H, Bruylants G (2019) J Colloid Interf Sci 557:807-15. doi: 10.1016/j.jcis.2019.09.047.
33. Liu G, Chockalingham M, Khor SM, Gui AL, Gooding JJ (2010) Electroanal 22:918-26. doi: 10.1002/elan.200900539.
34. Louault C, D'Amours M, Bélanger D (2008) ChemPhysChem 9:1164-70. doi: 10.1002/cphc.200800016.
35. Blond P, Bevernaegie R, Troian-Gautier L, Lagrost C, Hubert J, Reniers F, Raussens V, Jabin I (2020) Langmuir 36:12068-76. doi: 10.1021/acs.langmuir.0c02681.
36. Retout M, Blond P, Jabin I, Bruylants G (2021) Bioconjugate Chemistry 32:290-300. doi: 10.1021/acs.bioconjchem.0c00669.
37. Lenne Q, Mattiuzzi A, Jabin I, Le Poul N, Leroux YR, Lagrost C (2020) Adv Mater Interfaces 7:2001557. doi: 10.1002/admi.202001557.
38. Li X-M, Reinhoudt D, Crego-Calama M (2007) Chem Soc Rev 36:1350-68. doi: 10.1039/B602486F.
39. Wang S, Liu K, Yao X, Jiang L (2015) Chem Rev 115:8230-93. doi: 10.1021/cr400083y.
40. Yong J, Chen F, Yang Q, Huo J, Hou X (2017) Chem Soc Rev 46:4168-217. doi: 10.1039/C6CS00751A.

41. Kim A, Lee C, Kim H, Kim J (2015) ACS Appl Mater Interfaces 7:7206-13. doi: 10.1021/acsami.5b00292.
42. Howarter JA, Youngblood JP (2007) Adv Mater 19:3838-43. doi: 10.1002/adma.200700156.
43. Ragesh P, Anand Ganesh V, Nair SV, Nair AS (2014) J Mater Chem A 2:14773-97. doi: 10.1039/C4TA02542C.
44. Xiao F, Yuan S, Liang B, Li G, Pehkonen SO, Zhang T (2015) J Mater Chem A 3:4374-88. doi: 10.1039/C4TA05730A.
45. Zhang B, Zhao X, Li Y, Hou B (2016) RSC Adv 6:35455-65. doi: 10.1039/C6RA05484F.
46. Banerjee I, Pangule RC, Kane RS (2011) Adv Mater 23:690-718. doi: 10.1002/adma.201001215.
47. Le Poul N, Le Mest Y, Jabin I, Reinaud O (2015) Acc Chem Res 48:2097-106. doi: 10.1021/acs.accounts.5b00152.
48. Devouge S, Conti J, Goldsztein A, Gosselin E, Brans A, Voué M, De Coninck J, Homblé F, Goormaghtigh E, Marchand-Brynaert J (2009) J Colloid Interf Sci 332:408-15. doi: 10.1016/j.jcis.2008.12.045.
49. Nabers A, Ollesch J, Schartner J, Kötting C, Genius J, Haußmann U, Klafki H, Wiltfang J, Gerwert K (2016) J Biophotonics 9:224-34. doi: 10.1002/jbio.201400145.
50. Voue M, Goormaghtigh E, Homble F, Marchand-Brynaert J, Conti J, Devouge S, De Coninck J (2007) Langmuir 23:949-55. doi: 10.1021/la061627j.
51. Retout M, Valkenier H, Triffaux E, Doneux T, Bartik K, Bruylants G (2016) ACS Sensors 1:929-33. doi: 10.1021/acssensors.6b00229.
52. Lenne Q, Leroux YR, Lagrost C (2020) ChemElectroChem 7:2345-63. doi: 10.1002/celc.202000132.
53. Franco F, Rettenmaier C, Jeon HS, Roldan Cuenya B (2020) Chem Soc Rev 49:6884-946. doi: 10.1039/D0CS00835D.
54. Rodriguez P, Koper MTM (2014) Phys Chem Chem Phys 16:13583-94. doi: 10.1039/C4CP00394B.
55. Erikson H, Sarapuu A, Tammeveski K, Solla-Gullón J, Feliu JM (2014) ChemElectroChem 1:1338-47. doi: 10.1002/celc.201402013.